

# Nonlinear scattering of acoustic waves by vibrating surfaces<sup>a)</sup>

Jean C. Piquette and A. L. Van Buren

Naval Research Laboratory, Underwater Sound Reference Detachment, P. O. Box 8337, Orlando, Florida 32856

(Received 17 June 1983; accepted for publication 8 June 1984)

The problem of the scattering of acoustic waves by a vibrating surface surrounded by a fluid was investigated. Theoretical results were obtained for the specific case of a plane wave (of angular frequency  $\omega_p$ ) normally incident on an infinitely long cylinder vibrating uniformly and harmonically (at angular frequency  $\omega_c$ ) in the radial direction. This problem was previously studied by Censor [J. Sound Vib. 25, 101–110 (1972)], who used the linear equation together with nonlinear boundary conditions to obtain his solution. In addition to ordinary rigid-body scattering, Censor predicted nongrowing waves at the sum and difference frequencies  $\omega_p \pm \omega_c$ . However, medium nonlinearities also produce sum- and difference-frequency waves. The amplitudes of these waves tend to grow with increasing distance from the surface and, after a very small distance, dominate those predicted by Censor. In the present study, an expression for the difference-frequency wave was obtained using the simple-source formulation of the nonlinear wave equation subject to the appropriate boundary conditions. The expression was evaluated numerically for specific parameters and the results are presented graphically. Efforts to experimentally confirm the theoretical predictions were inhibited by the presence of previously unsuspected levels of hydrophone nonlinearity.

PACS numbers: 43.25.Gf, 43.25.Jh, 43.20.Tb, 43.25.Cb

## INTRODUCTION

In 1972 Censor<sup>1</sup> considered the problem of the scattering of acoustic waves (of angular frequency  $\omega_p$ ) by a surface vibrating sinusoidally (at angular frequency  $\omega_c$ ). Censor solved the linear wave equation subject to a nonlinear boundary condition. In addition to the usual rigid-body scattered waves, Censor predicted waves at the sum and difference frequencies  $\omega_p \pm \omega_c$ . Shortly after the appearance of Censor's article, Rogers<sup>2</sup> pointed out that medium nonlinearities also would produce contributions to the sum- and difference-frequency components. Since the boundary effect predicted by Censor depends on the Mach number to the same order as the medium nonlinearities, any solution involving the sum- and difference-frequency components must necessarily involve the nonlinear wave equation.

In Sec. I we use the simple-source formulation of the nonlinear wave equation to solve the problem of a plane wave normally incident on an infinitely long cylinder vibrating uniformly and harmonically in the radial direction. Section II presents in graphical form the results obtained by numerically evaluating the solution for the specific case that was examined experimentally and compares them with Censor's results for the same problem. Section III describes the experimental investigation of this problem. It also discusses the unexpectedly high levels of nonlinearity that occurred in all the hydrophones tested. (This hydrophone nonlinearity precluded experimental confirmation of the theory.) Section

IV gives the conclusions. Finally, the Appendix gives a derivation of the simple-source formulation of the second-order nonlinear wave equation for arbitrary primary fields.

## I. PLANE-WAVE SCATTERING BY A VIBRATING CYLINDER

We consider the problem of calculating the sum- and difference-frequency acoustic waves produced when a plane wave (of angular frequency  $\omega_p$ ) is normally incident on an infinite cylinder vibrating harmonically (at angular frequency  $\omega_c$ ) and uniformly in the radial direction (see Fig. 1). (The solutions for some other geometries are given in Ref. 3.) The boundary conditions involve the assumption of "rigid-body oscillation" of the cylindrical surface (i.e., this surface vibrates only at the frequency  $\omega_c$  to all orders), and we require only outwardly propagating second-order fields. The pri-

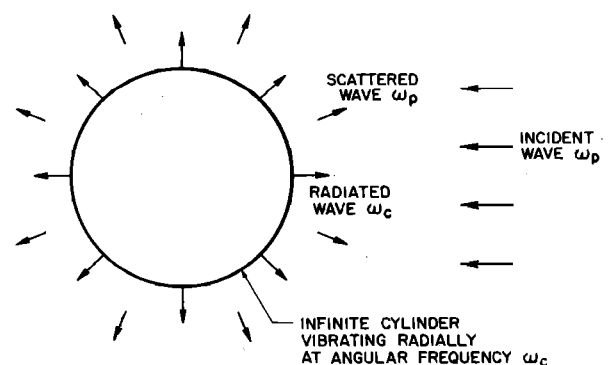


FIG. 1. Geometry of plane-wave scattering from a vibrating cylinder.

<sup>a)</sup>This article is based on the first author's Ph.D. thesis submitted to the faculty of the Stevens Institute of Technology in partial fulfillment of the degree requirements.

many sound sources are assumed to be operated at or near their fundamental resonance frequencies. We choose to express the problem in terms of the simple-source formulation of the nonlinear wave equation:

$$\square^2 P_2 = -\rho_0 \frac{\partial q}{\partial t}, \quad (1)$$

where  $q$  is the simple-source strength  $= (\Gamma / \rho_0^2 c_0^4) (\partial / \partial t) P_1^2$ ,  $\rho_0$  is the ambient density of the fluid,  $c_0$  is the small signal sound speed in the fluid,  $P_1$  is the primary-wave (first-order) pressure,  $P_2$  is the secondary-wave (second-order) pressure, and  $\Gamma$  is the nonlinearity parameter  $= 1 + (B/2A)$  with  $B/A = (\rho_0/c_0^2) (\partial^2 P / \partial p^2)_{S, \rho = \rho_0}$  (where  $S$  is the entropy). Westervelt<sup>4</sup> derived the simple-source formulation of Eq. (1) in 1963 under the assumption of plane waves for the primary pressure  $P_1$ . We rederived the formulation for arbitrary primary waves and obtained the same result. The derivation is provided in the Appendix.

For the present problem, the first-order pressure  $P_1$  is the sum of the incident plane wave  $P_{\text{plane}}$ , the wave  $P_{\text{scatt}}$  that is scattered when the plane wave is incident on the cylinder, and the wave  $P_{\text{cyl}}$  that is radiated by the vibrating cylinder. The cylinder may properly be considered a rigid scatterer providing the frequency of the incident plane wave is significantly below the lowest resonance frequency of the cylinder.<sup>5</sup> We assume this to be the case and obtain, using conventional linear theory:

$$\begin{aligned} P_1 &= P_{\text{plane}} + P_{\text{cyl}} + P_{\text{scatt}} \\ &= P_0 \left( J_0(k_p r) + 2 \sum_{m=1}^{\infty} i^m \cos(m\theta) J_m(k_p r) \right) \\ &\quad \times e^{-i\omega_p t} + A H_0(k_c r) e^{-i\omega_c t} \\ &\quad + \sum_{m=0}^{\infty} A_m \cos(m\theta) H_m(k_p r) e^{-i\omega_p t}, \end{aligned} \quad (2)$$

where  $P_0$  is the pressure amplitude of the incident plane wave,  $A$  is the pressure amplitude of the radiated cylindrical wave,  $J_m$  is the  $m$ th-order cylindrical Bessel function of the first kind,  $H_m$  is the  $m$ th-order cylindrical Hankel function of the first kind,  $a$  is the cylinder radius,  $A_m$  is the  $m$ th rigid-body scattering coefficient,<sup>6</sup> and  $k = \omega/c_0$  is the wavenumber. We have expressed the plane wave in terms of its expansion in cylindrical coordinates.

In order to obtain the sum- and difference-frequency components ( $\omega_{\pm} = \omega_p \pm \omega_c$ ) of the second-order pressure  $P_2$ , we begin by obtaining the corresponding frequency terms in the simple-source term  $\rho_0 (\partial q / \partial t)_{\pm}$ . Since both the sum- and difference-frequency cases can be handled in a similar fashion, we will describe in detail only the calculation of the difference-frequency component. We suppress the time dependence  $\exp(-i\omega_{-} t)$  and obtain the following equation for the time-independent amplitude of the difference frequency  $P_{-}(r') \equiv P_{-}(r, \theta)$ :

$$\nabla^2 P_{-}(r, \theta) + k_{-}^2 P_{-}(r, \theta) = B_{-}(r, \theta), \quad (3)$$

where  $B_{-}(r, \theta)$  is the time-independent amplitude of the difference-frequency component of the simple-source term. We define a Green's function associated with Eq. (3),  $G_{-}(r, r')$ , such that:

$$\nabla^2 G_{-}(r, r') + k_{-}^2 G_{-}(r, r') = -\delta(r - r'), \quad (4)$$

where  $\delta(r - r')$  is the Dirac delta function. To be consistent with our assumption that the cylinder is a rigid-body scatterer at the difference frequency, the normal derivative of  $G_{-}(r, r')$  is required to vanish on the cylindrical surface.

A representation for  $P_{-}$  may be obtained by multiplying Eq. (4) by  $B_{-}$  and Eq. (3) by  $G_{-}(r, r')$ , subtracting the resulting equations, and integrating over primed variables. The result is

$$\begin{aligned} P_{-}(r) &= - \int d\tau' B_{-}(r') G_{-}(r, r') \\ &\quad + \iint G_{-}(r, r') \nabla P_{-}(r', \theta') \cdot dS', \end{aligned} \quad (5)$$

where the vanishing of the normal gradient of the Green's function has been imposed.

We now consider the surface integral in Eq. (5), focusing our attention first on the  $\nabla P_{-}$  term of the integrand. If the current problem was being solved in Lagrangian coordinates, this term would vanish. In Lagrangian coordinates the proportionality between the pressure gradient and the velocity is exact (due to the form of the equation of motion). Hence,  $\nabla P_{-}$  would be proportional to the surface velocity at the difference frequency and, therefore, equal to zero due to the rigid-body boundary condition. The current problem is actually being solved in Eulerian coordinates. However, an upper bound for the contribution to  $P_{-}(r)$  from this surface integral can still be estimated using plane waves. (This has been done in Ref. 3.) The result is that the surface integral contributes negligibly to the difference-frequency pressure (in all directions) at radial distances exceeding one difference-frequency wavelength. We choose, therefore, to neglect this surface integral and to represent  $P_{-}(r)$  simply as

$$P_{-}(r) = - \int d\tau' B_{-}(r') G_{-}(r, r'). \quad (6)$$

The rigid-body Green's function appropriate to cylindrical geometry is well known<sup>7</sup> and is given for the region  $r' < r$  by

$$\begin{aligned} G_{-}(r, r') &= \frac{i}{4} \sum_{m=0}^{\infty} \epsilon_m \cos m(\phi - \phi') \left( H_m(k_{-} r) J_m(k_{-} r') \right. \\ &\quad \left. - \frac{J'_m(k_{-} a)}{H'_m(k_{-} a)} H_m(k_{-} r) H_m(k_{-} r') \right), \end{aligned} \quad (7)$$

where  $\epsilon_m = 1$  if  $m = 0$ ,  $\epsilon_m = 2$  if  $m \neq 0$ , and primes on the Bessel functions denote differentiation with respect to the argument. The corresponding Green's function for the region  $r' > r$  is not needed since contributions to the integral of Eq. (5) from this region (which is further radially from the source than the point of interest) will be assumed negligible. These contributions do not add up constructively but tend to cancel each other due to phase mismatching. Conversely, contributions from the region  $r' < r$  tend to add constructively and provide essentially the entire difference-frequency wave present at the observation point. (Estimates of the small errors involved in restricting the integration to  $r' < r$  are provided in Ref. 3.)

The simple-source term of Eq. (1) involves the square of the first-order field  $P_1^2$ . The difference-frequency compo-

ment of the quantity  $P_1^2$  can be calculated using Eq. (2). We must, however, use only the real part of  $P_1$  when forming quadratic terms in order to avoid introducing erroneous contributions. Expressed in complex notation for convenience, the resulting amplitude  $B_-$  of the difference-frequency component of  $P_1^2$  is given by

$$B_-(r, \theta) = -2(\omega_p - \omega_c)^2 A \Gamma \left( P_0 H_0(k_c r) J_0(k_p r) + \sum_{m=0}^{\infty} A_m^* \cos(m\theta) H_0(k_c r) H_m(k_p r) + 2 \sum_{m=1}^{\infty} P_0 i^{-m} \cos(m\theta) H_0(k_c r) J_m(k_p r) \right), \quad (8)$$

where the asterisk denotes complex conjugates. Equation (8)

$$P_-(r) = \frac{-\pi i P_0 (\omega_p - \omega_c)^2 A \Gamma}{2\rho_0 c_0^4} \left[ H_0(k_d r) \left( \int_a^r dr' r' H_0^*(k_c r') J_0(k_p r') J_0(k_d r') - \frac{J_0'(k_d a)}{H_0'(k_d a)} \int_a^r dr' r' H_0^*(k_c r') J_0(k_p r') H_0(k_d r') \right) + \sum_{l=0}^{\infty} \left( \frac{A_l}{P_0} \right) \cos(l\theta) H_l(k_d r) \left( \int_a^r dr' r' H_0^*(k_c r') H_l(k_p r') J_l(k_d r') - \frac{J_l'(k_d a)}{H_l'(k_d a)} \int_a^r dr' r' H_0^*(k_c r') H_l(k_p r') H_l(k_d r') \right) + 2 \sum_{l=1}^{\infty} i^l \cos(l\theta) H_l(k_d r) \left( \int_a^r dr' r' H_0^*(k_c r') J_l(k_p r') J_l(k_d r') - \frac{J_l'(k_d a)}{H_l'(k_d a)} \int_a^r dr' r' H_0^*(k_c r') J_l(k_p r') H_l(k_d r') \right) \right]. \quad (9)$$

## II. NUMERICAL RESULTS

In order to illustrate the solution given in Eq. (9), as well as the corresponding solution given by Censor,<sup>1</sup> we used parameter values that were experimentally realizable to make example calculations. We chose the plane-wave frequency to be 162 kHz and the cylindrical-wave frequency to be 102 kHz, thus obtaining a difference frequency of 60 kHz. We chose the amplitude of the incident pressure wave to be  $1.0 \times 10^5$  Pa and the cylindrical-wave amplitude coefficient  $A$  equal to  $3.5 \times 10^5$  Pa. Water was chosen for the surrounding fluid.

We first numerically evaluated Censor's solution for this case. His solution, given by Eqs. (5), (10), (23), and (24) of Ref. 1 is a relatively simple Bessel function series. The resulting angular distribution of difference-frequency pressure at 15 cm from the symmetry axis of the cylinder is shown in Fig. 2. The maximum pressure at this radius occurs at  $\theta = 0^\circ$  and is equal to 0.9 Pa. (In Fig. 2, as well as in all following polar plots, the dB scale is measured relative to the maximum pressure value at the radius of interest. The maximum pressure value corresponding to a particular polar diagram is given in the information box associated with it and is referred to as " $P_{MAX}$ ." Additionally, the symbol  $\nu_p$  represents the frequency of the incident plane wave,  $\nu_c$  represents the frequency of the radiated cylindrical wave, and  $\nu_d$  represents the difference frequency.) As expected, the pressure values predicted by Censor's theory turn out to be of the same order of magnitude as pseudosound<sup>2</sup>; i.e., they are comparable to the difference-frequency component obtained by transforming the sum of the primary fields present at the observation point from Lagrangian to Eulerian coordinates (or vice versa).

is the proper form for  $B_-$  only when  $\omega_p > \omega_c$ . If  $\omega_c > \omega_p$ , the correct form for  $B_-$  is the complex conjugate of the right-hand side of Eq. (8). In the following analysis, we chose  $\omega_p > \omega_c$ , since this case was easier to implement experimentally. (Unfortunately the assumption that the cylinder is acoustically rigid at the primary frequency  $\omega_p$  is questionable when  $\omega_p > \omega_c$  so that the rigid-body scattering coefficients are probably inappropriate. However, an empirical set of scattering coefficients  $A_m$ , determined by directly measuring the linearly scattered field, may be used instead.)

We obtain the difference-frequency pressure  $P_-(r)$  by substituting the expression for  $B_-(r')$  given by Eq. (8) and the Green's function  $G_-(r, r')$  of Eq. (7) into Eq. (6). The integrals over  $\theta$  may be performed easily to provide the following expression for the difference-frequency pressure:

The behavior of the difference-frequency pressure with respect to radial distance from the cylinder symmetry axis is shown in Fig. 3 for  $\theta = 0^\circ$  (a similar behavior is seen at other angles). This graph can be interpreted in the following way:

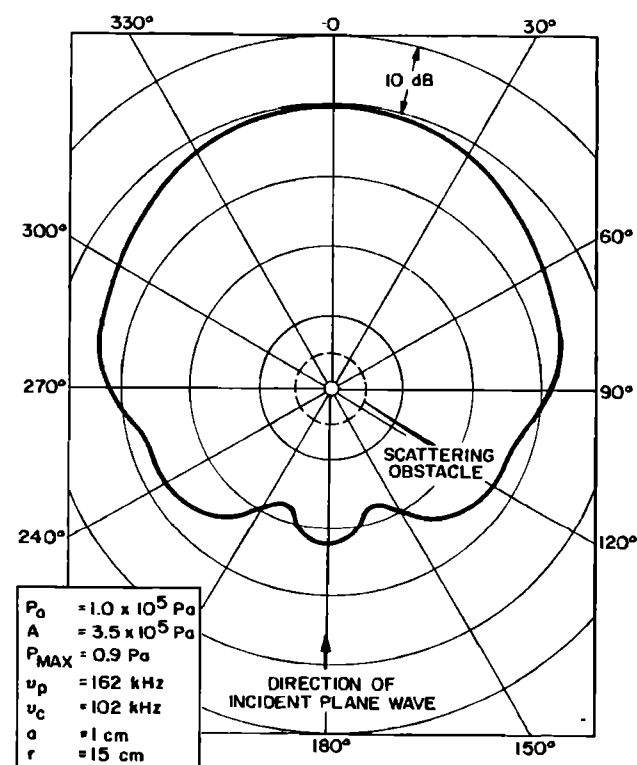


FIG. 2. Angular distribution of the difference-frequency pressure as predicted by the Censor theory<sup>1</sup> for a radial distance of 15 cm.

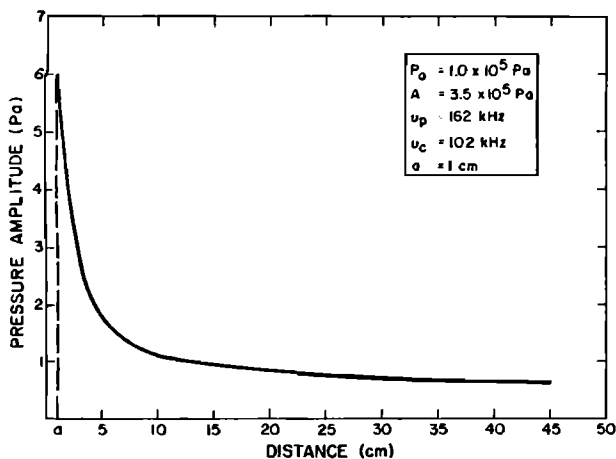


FIG. 3. Radial distribution of difference-frequency pressure as predicted by the Censor theory<sup>1</sup> for  $0^\circ$ .

Censor's theory predicts the generation of difference-frequency waves (as well as sum-frequency waves) due to the presence of *boundary conditions* associated with the time-varying nature of the cylindrical surface. Hence, both the sum- and difference-frequency waves predicted by his theory are created solely at the surface of the scatterer. As the observation point is moved to increasingly greater distances from the boundary, these sum- and difference-frequency pressure waves must spread cylindrically (in a manner similar to the spreading of the first-order cylindrical field). In the asympto-

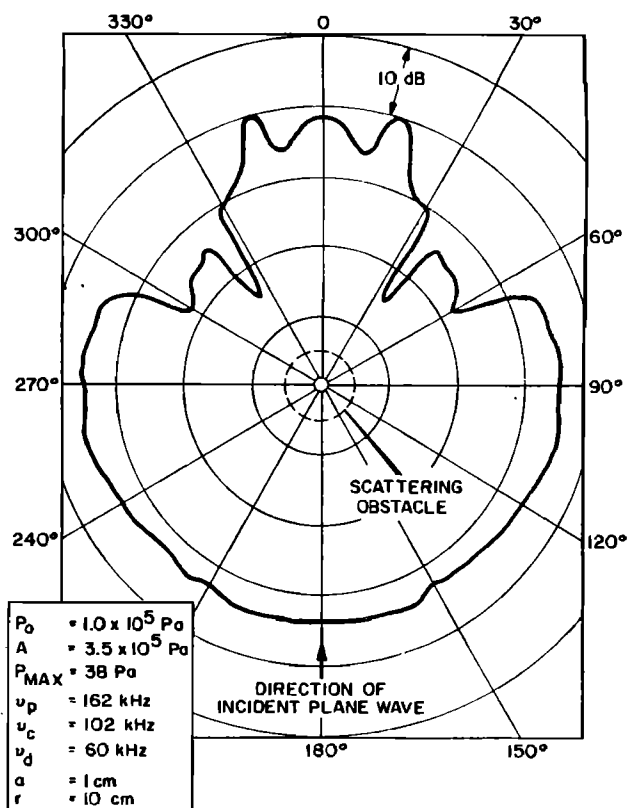


FIG. 5. Angular distribution of the nonlinearly generated difference-frequency pressure at a radial distance of 10 cm.

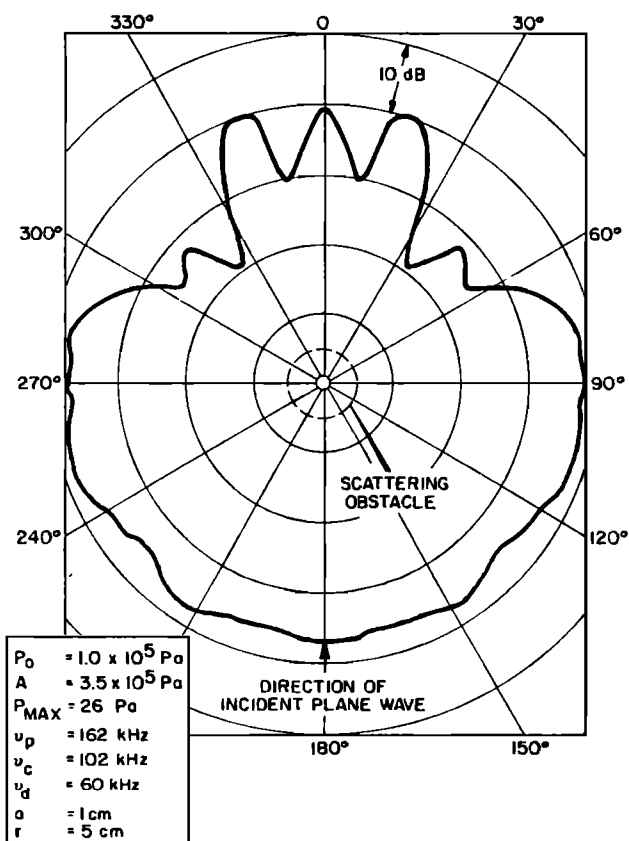


FIG. 4. Angular distribution of the nonlinearly generated difference-frequency pressure at a radial distance of 5 cm.

tic limit their magnitude will decrease inversely as the square root of the radial distance from the symmetry axis. This behavior is seen in Fig. 3.

The solution to the nonlinear wave equation for this problem is given by Eq. (9). This solution contains complicated integrals involving triple products of Bessel functions. We developed a new technique of integration<sup>9</sup> suitable for evaluating these integrals for the special case in which the argument of the Bessel functions corresponding to the radiated cylindrical wave as well as the argument of the Bessel functions corresponding to either the incident plane wave *or* the difference-frequency wave are sufficiently large for the Bessel functions to be replaced by their asymptotic forms. Unfortunately, these conditions were not met for the present example so we evaluated the integrals numerically instead of by the use of Gaussian quadrature.

The resulting angular distributions of the difference-frequency pressure calculated using Eq. (9) for radial distances of 5, 10, and 15 cm from the scatterer's center are presented in Figs. 4, 5, and 6, respectively. These graphs may be interpreted qualitatively in the following way: For angles near  $0^\circ$ , strong contributions to the difference-frequency pressure are obtained from the "mixing" of both the incident plane wave and the rigid-body scattered wave with the cylindrically radiated wave. Since the cylindrically radiated wave does not vary with angle, the variation of difference-frequency pressure with angle near  $0^\circ$  should be similar to that of the sum of the incident plane-wave pressure and the rigid-body scattered pressure; i.e., of the total linear pressure field for

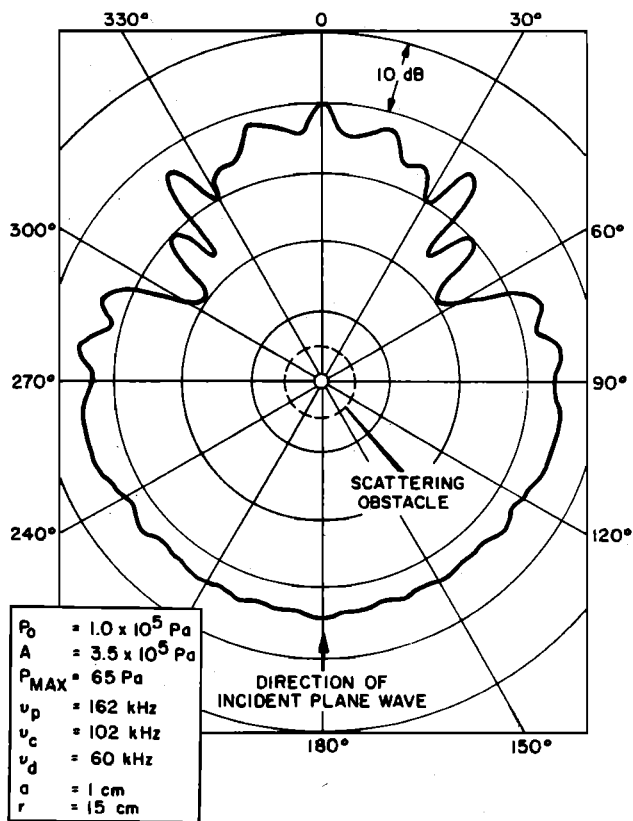


FIG. 6. Angular distribution of the nonlinearly generated difference-frequency pressure at a radial distance of 15 cm.

rigid-body scattering. Figure 7 presents the angular distribution of the total pressure field at 15 cm (the distribution is not significantly different at points closer to the scatterer's surface). It is interesting to note that peaks are present in this field at 0° and 15°, corresponding closely to peaks in the difference-frequency field.

At angles not near 0°, the incident plane wave no longer strongly contributes to the difference-frequency field. Hence, for these angles, the angular dependence of the rigid-body scattered pressure alone is more appropriate for understanding the angular dependence of the difference-frequency pressure. The angular distribution of the rigid-body scattered pressure at 15 cm is presented in Fig. 8. (Again, the distribution is not significantly different at points closer to the scatterer's surface.) A significant feature in the difference-frequency distribution of Figs. 4–6 is a pressure level that is nearly constant for angles between approximately 60° and 300°. This corresponds well to the distribution of Fig. 8 with the exception of narrow notches appearing there at approximately 75°, 135°, 225°, and 285°. These notches are so narrow that their effect tends to “wash out” in the integrated result for the difference-frequency pressure.

The difference-frequency distribution for angles between 15° and 60° and between 300° and 345° do not correspond closely to either Fig. 7 or 8. The maxima and minima occurring here arise due to *linear interference* between the two nonlinearly generated difference-frequency component waves of the second-order field. One difference-frequency component arises from the interaction of the incident plane wave with the cylindrically radiated wave. The other compo-

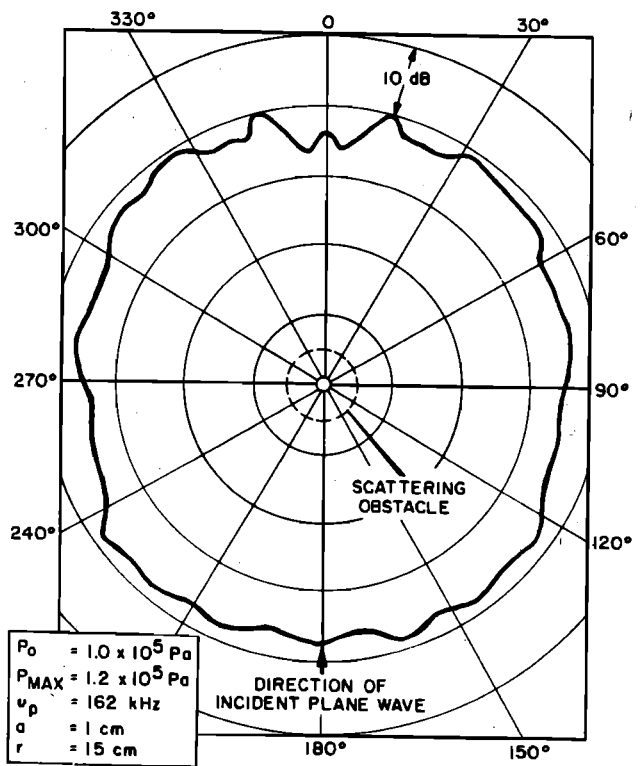


FIG. 7. Angular distribution of the total linear pressure at 162 kHz at a radial distance of 15 cm.

nent arises from interaction of the rigid-body scattered wave with the cylindrically radiated wave. The variations in pressure amplitude apparent in the angular intervals 15° through 60° and 300° through 345° result from phase differences

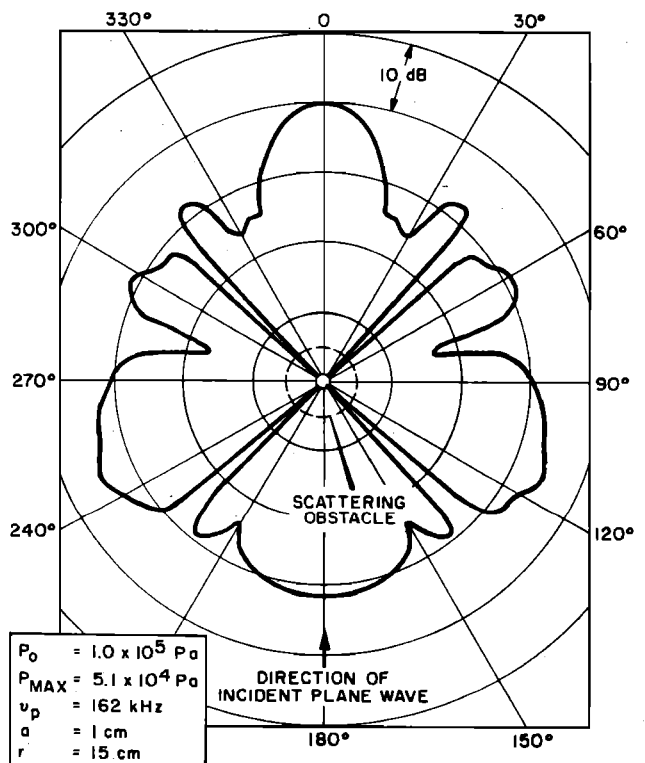


FIG. 8. Angular distribution of linearly scattered pressure at 162 kHz at a radial distance of 15 cm.

between the two components that vary rapidly with observation angle. On the other hand, at observation angles near  $0^\circ$ , the relative phase angle does not vary rapidly. Hence, as previously discussed, the angular distribution of difference-frequency pressure near  $0^\circ$  is similar to the angular distribution of the total linear pressure field, even though the two nonlinear components are comparable in magnitude. Similarly, at large observation angles the difference-frequency pressure arising from the interaction of the incident plane wave with the cylindrically radiated wave is quite small; hence, the angular distribution of the rigid-body scattered pressure alone may properly be used to understand the angular distribution of the difference-frequency pressure.

We present the behavior of the difference-frequency pressure as a function of radial distance at angles of  $0^\circ$ ,  $90^\circ$ , and  $180^\circ$  in Figs. 9, 10, and 11, respectively. We note in Fig. 9 that for  $\theta = 0^\circ$  the difference-frequency pressure increases approximately linearly with increasing distance. This growth is similar to that obtained for the parametric array<sup>4</sup> when a single piston source is driven at two different primary frequencies. The similarity is understandable since the incident plane wave acts exactly as one of the primary waves does in the parametric array and the radiated cylindrical waves approximates the behavior of the second primary.

At angles not near  $0^\circ$ , however, significant contributions to the difference-frequency pressure come primarily from mixing of the rigid-body scattered wave with the cylindrically radiated wave. Since the rigid-body scattered wave also spreads cylindrically, the interaction between these two waves is similar to the interaction of two concentric cylindrically radiated waves. This problem was considered by Dean,<sup>10</sup> who showed that, unlike the parametric array, the difference-frequency wave generated in this case approaches a constant amplitude as the observation point approaches the farfield. This same behavior occurs in the present problem as is seen in Figs. 10 and 11.

Thus comparison of Figs. 3 and 9 shows that the nonlinear volume effect rapidly overwhelms the surface effect of Censor.<sup>1</sup> Similar results were obtained for other angular directions, downshift ratios, and for the other geometrical configurations discussed in Ref. 3.

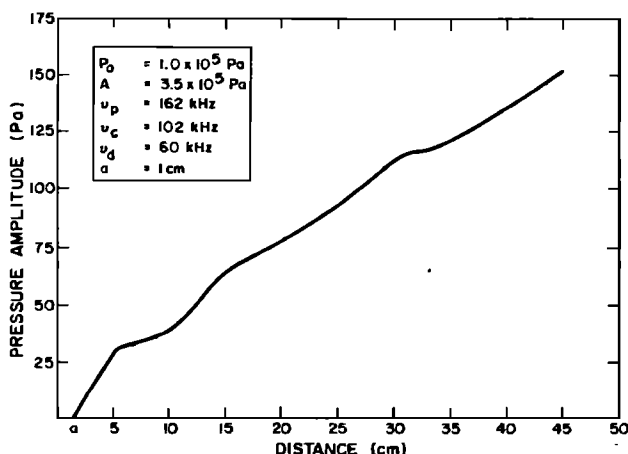


FIG. 9. Radial distribution of the nonlinearly generated difference-frequency pressure for  $0^\circ$ .

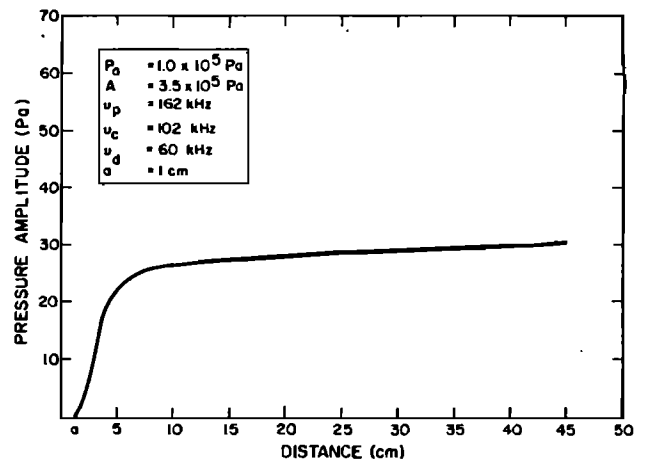


FIG. 10. Radial distribution of the nonlinearly generated difference-frequency pressure for  $90^\circ$ .

### III. EXPERIMENT

We attempted to confirm the theoretical predictions by performing an experimental investigation. We used an air-backed piston transducer containing a lead-zirconate-titanate disk 12.7 cm in diameter and 1.27 cm thick for the source of plane waves. The fundamental resonance frequency of this transducer was measured to be 162 kHz. The cylindrical-wave source consisted of eight piezoelectric rings (o.d. = 2 cm, i.d. = 0.938 cm; length = 1.905 cm) coaxially mounted to create a line 15.24 cm long. This transducer was determined to have a breathing mode resonance at 102 kHz. Since this transducer was not expected to be a rigid-body scatterer at 162 kHz, we replaced the theoretical rigid-body scattering coefficients with an empirical set extracted from the measured linearly scattered field at 162 kHz and computed new theoretical results for comparison with experiment. A USRD standard hydrophone (type F42D) was used as the acoustic sensor for most measurements. It was mounted so that it could be revolved in a circle centered on the cylindrical source and in a plane perpendicular to the symmetry axis of the cylindrical source (see Fig. 12).

During the investigation several fundamental experimental difficulties arose. Previous experiments involving

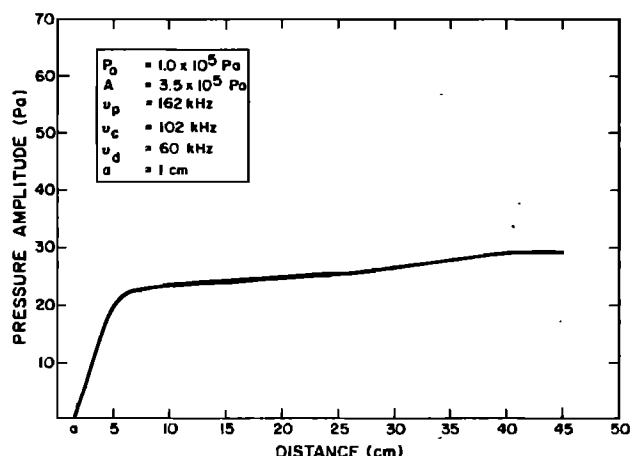


FIG. 11. Radial distribution of the nonlinearly generated difference-frequency pressure for  $180^\circ$ .

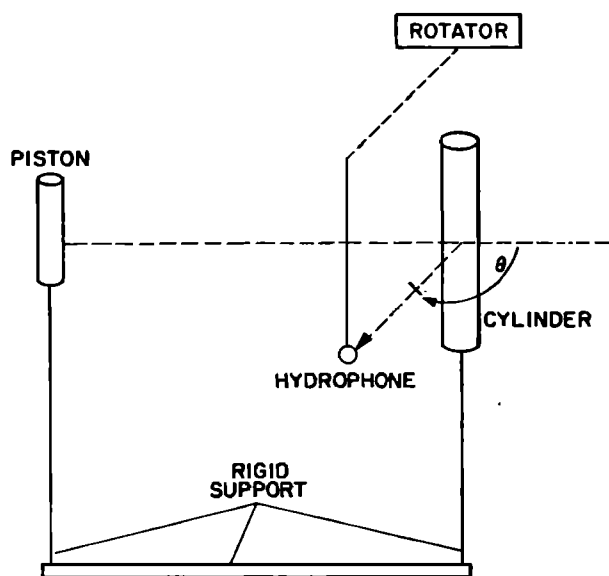


FIG. 12. Measurement geometry for the nonlinear scattering experiment and for the new method of nonlinear hydrophone calibration.

two high amplitude primary waves interacting nonlinearly in a fluid medium could often be designed to avoid these difficulties. The present experiment could not be designed to avoid them. The most important of these difficulties are discussed in Secs. III A–C.

#### A. Inadvertent direct radiation of the sources at the difference frequency

Since the sources are naturally finite in extent, measurements must be made in the extreme nearfield of the sources in order to approximate an infinite plane wave and infinitely long cylinder. Direct radiation by the sources at the difference frequency tends to decrease with increasing distance while the nonlinearly generated difference-frequency wave tends to increase. Hence, direct radiation tends to be a greater source of error in the nearfield than when the measuring hydrophone is far from the sources. We had to use moderately short acoustic pulses in our experiment in order to avoid interfering reflections from neighboring surfaces. When we drove the cylinder and piston with electrical pulses with the conventional rectangular-envelope shape, the resulting directly radiated difference-frequency component was unacceptably large. Fortunately, this difficulty was fairly straightforward to eliminate. By passing each of the electrical pulses through special pulse-shaping networks that were designed to reduce the difference-frequency component in the envelope, 95% of the directly radiated difference-frequency component was eliminated. Prior to the addition of these networks, the directly radiated difference-frequency component was comparable in magnitude to that expected to be generated nonlinearly in the water. After the addition of the network, the direct radiation became a small component of the total difference-frequency pressure field.

#### B. Electrical filtering problems due to experimental constraints

The pulse lengths used in the experiment had to be less than about ten cycles at the difference frequency to avoid

interfering reflections from neighboring surfaces (the pulses could not have been substantially shorter than this, however, because of sound source turn-on transients). In addition, the difference frequency was only about one-half the lowest primary frequency. Hence, the passive methods usually employed for electrical filtering in nonlinear measurements are inadequate. This difficulty was resolved by the selection of extremely linear state-of-the-art active electrical filters. Previous nonlinear measurements were not faced with this problem. First of all, earlier measurements were made at least moderately far from the sources or did not involve multiple sources and did not involve the possibility of unwanted single or multiple reflections. Long pulse lengths could be used without interfering reflections being received, and a passive filter could be used. Since passive filters are generally far more linear than active filters, nonlinear generation in these filters did not present a problem. In addition, highly effective low-pass filters can be designed for passive operation (even more effective than active filters due to lower internal noise) when one can tolerate the attendant long turn-on transients. Secondly, since large downshift ratios (i.e., the ratio of the average primary frequency to the difference frequency) were often used in previous work (typically greater than 10 as opposed to 2.2 in our case), the filters did not have to be able to separate a very small amplitude difference-frequency component from large primaries that are not very different in frequency.

In order to assure that no appreciable difference-frequency component was being generated nonlinearly in the active filters chosen in this work, a mixing amplifier was used to electrically add two electrical signals of the same frequencies as those of the two primaries used in the experiment. The voltage amplitudes of these electrical signals were chosen to be comparable to the voltage amplitudes arising from the hydrophone's linear response to the primary pressures. No difference-frequency component could be measured under these conditions except for that associated with the electrical noise floor of the receiving system. The equivalent acoustic pressure at the difference frequency corresponding to this noise is about 27 Pa, which is one-half the theoretically predicted difference frequency in the forward direction at just 6 cm from the center of the cylinder. The signal produced nonlinearly in the water continues to grow approximately linearly in this direction with increasing radial distance. Although the receiving system noise is large enough to prevent precise definitive measurements of the difference-frequency component close to the cylinder, it becomes unimportant at greater distances (at least in the  $\theta = 0^\circ$  direction).

#### C. Difference-frequency voltage generated nonlinearly in the hydrophone's sensitive element

This effect, due to mechanical nonlinear mixing of the primaries in the hydrophone, provided larger difference-frequency voltages than those produced by the hydrophone's linear response to the difference-frequency pressure generated nonlinearly in the water. The effect was observed for a wide range of available hydrophones. At the time we began the experimental investigation, no one even suspected that

hydrophones were nonlinear to a measurable degree. Recently, however, a study of hydrophone nonlinearity was performed jointly by researchers at the Naval Underwater Systems Center and the Underwater Sound Reference Detachment of the Naval Research Laboratory.<sup>11,12</sup> Initially we hoped that the results of their measurements, which were performed at a high downshift ratio in the nearfield of a piston source driven at two frequencies, could be extrapolated to our case of a small downshift ratio and nonparallel primary waves. The extrapolation predicted a hydrophone nonlinearity that was small enough to allow the experiment to be carried out, at least at field points where the difference-frequency pressure generated nonlinearly in the water was relatively large. Unfortunately, when the nonlinear responses of the hydrophones used in the experiment were measured by a different technique, one more appropriate to our case, they proved to be substantially more nonlinear, so much so as to prevent any accurate measurements of difference-frequency pressure in our experiment.

In addition to finding that the nonlinearity calibration measurements of Refs. 11 and 12 could not be extrapolated for our experimental conditions, it was discovered that the nonlinear response of a hydrophone is extremely sensitive to the geometry of incidence of the primary waves upon its active elements. In order to understand this, it is helpful to first consider the experimental configuration of the nonlinearity measurement as shown in Fig. 12. The piston and cylinder sound sources were held in fixed positions, while the hydrophone was rotated in a circle (of radius  $x$ ) centered on the cylinder axis and in a plane perpendicular to the plane of the drawing. (The piston source was located a distance  $2x$  from the cylinder's symmetry axis.) As the hydrophone was moved through its measurement path, its *linear* response to the pressure fields created by the piston and the cylinder (driven at different frequencies) was monitored. Simultaneously, the hydrophone's difference-frequency voltage output was recorded. This difference-frequency voltage was on the average about an order of magnitude greater than would be expected from the hydrophone's linear response to the difference-frequency pressure present in the water as predicted by the nonlinear theory presented in Sec. I. Hence, the vast majority of the observed difference-frequency voltage detected arose from the nonlinear response of the hydrophone itself. (Several different piezoelectric hydrophones were tested in this way, and *all* exhibited difference-frequency voltages far in excess of that predicted by the nonlinear theory.) As the hydrophone was revolved through its circular path, there were certain angular positions at which the received voltages of each of the primaries was seen to *decrease*, while the difference-frequency voltage was observed to increase. We conclude that the nonlinear response of the hydrophone is very sensitive to the relative angle of incidence of the primary waves on the hydrophone face.

In order to be certain that the observed difference-frequency voltage was in fact due to hydrophone self-nonlinearity (and did not arise from interaction of the primaries in the water), the hydrophone was moved to the  $\theta = 180^\circ$  (backscatter) direction (see Fig. 12). The primaries in this direction are propagating in opposite directions; hence, they do not

produce the well-known cumulative parametric effect (owing to unfavorable phase conditions of each primary relative to the other). Additionally, it was possible (using appropriate gating techniques) to observe the difference-frequency voltage output of the hydrophone before the primaries overlapped significantly, further reducing the likelihood that this voltage arose due to interaction of the primaries in the water. Even under these conditions, the observed difference-frequency voltage was approximately an order of magnitude greater than the value predicted theoretically for nonlinear backscatter from the cylindrical source. We conclude that the measured difference-frequency voltage is primarily due to the nonlinearity of the hydrophone itself.

#### IV. CONCLUSIONS

The simple-source formulation of the nonlinear wave equation has been rederived for arbitrary primary fields. The problem of the nonlinear scattering of acoustic waves by vibrating surfaces was solved using this equation for the case of a plane wave normally incident on an infinitely long cylinder vibrating uniformly and harmonically in the radial direction. In particular, an expression was obtained for the pressure of the difference-frequency wave produced by the nonlinear interaction of the cylindrically radiated wave with both the incident plane wave and its rigid-body scattered wave. The resulting expression was numerically evaluated using a digital computer, and the results are presented graphically. The difference-frequency pressure calculated using the nonlinear wave equation is substantially larger than that calculated based on the theory of Censor,<sup>1</sup> which is based on use of the linear wave equation together with nonlinear boundary conditions. Attempts to experimentally confirm the theoretical predictions were precluded by previously unsuspected levels of nonlinearity in the hydrophones used. It was determined that the nonlinear response of a piezoelectric hydrophone is extremely sensitive to both the downshift ratio and to the geometry of incidence of the primary waves on its active elements.

#### ACKNOWLEDGMENTS

The authors gratefully acknowledge valuable technical discussions with Professor H. Salwen of Stevens Institute of Technology and Dr. P. H. Rogers of Georgia Institute of Technology. We also acknowledge the valuable efforts of G. Hansen of the Underwater Sound Reference Detachment of the Naval Research Laboratory in designing and building the pulse-shaping networks used in our experiment.

#### APPENDIX: DERIVATION OF THE SIMPLE-SOURCE FORMULATION OF THE SECOND-ORDER NONLINEAR WAVE EQUATION FOR ARBITRARY PRIMARY FIELDS

A second-order nonlinear wave equation was derived in 1948 by Eckart<sup>13</sup> and later by Westervelt.<sup>14</sup> In 1963 Westervelt<sup>4</sup> transformed this equation into a form known as the simple-source formulation. However, he used the relation  $P = \rho_0 c_0 \mu$  in his derivation, which is strictly valid only for plane waves. He introduced this relation immediately following his Eq. (6) of Ref. 4. Westervelt's Eq. (6) may be written

$$\square^2 P = -\frac{1}{2} c_0^{-6} \left( \frac{\partial^2 P}{\partial \rho^2} \right)_{s, \rho = \rho_0} \frac{\partial^2 (P)^2}{\partial t^2} - \rho_0^2 \nabla^2 u + \square^2 \left[ \frac{1}{2} \rho_0 u^2 + \frac{1}{2} c_0^2 (\Delta \rho)^2 / \rho_0 \right], \quad (\text{A1})$$

where we have retained the D'Alembertian terms discarded by Westervelt and use  $P$  to represent the total acoustic pressure (instead of resolving it into primary and secondary waves as was done there).

In order to carry Eq. (A1) further it is useful to first introduce the usual first-order definition of the velocity potential,  $\mathbf{u} = -\nabla\phi$ , where  $\phi$  satisfies the first-order equation  $\square^2\phi = 0$ . (As has been pointed out by Blackstock,<sup>15</sup> any quadratic term may freely be replaced by its first-order equivalent without destroying the second-order accuracy of an equation. This is because any more accurate substitution would result in terms of higher than second order. This principle, used by Lighthill,<sup>16</sup> was called the "substitution corollary" by Blackstock. We use this corollary freely throughout the derivation.) By rearranging the definition of the D'Alembertian, it is easy to show that, to second order,

$$\nabla^2 u^2 = \square^2 u^2 + c_0^{-2} \frac{\partial^2}{\partial t^2} |\nabla\phi|^2. \quad (\text{A2})$$

Similarly, by rearranging the definition of the D'Alembertian operator acting on  $\phi$  and on  $\phi^2$ , along with Eq. (A2), we obtain (again, accurate to second order)

$$\nabla^2 u^2 = \square^2 u^2 + c_0^{-2} \frac{\partial^2}{\partial t^2} \left[ \frac{1}{2} \square^2 \phi^2 + c_0^{-2} \left( \frac{\partial\phi}{\partial t} \right)^2 \right]. \quad (\text{A3})$$

At this point we wish to re-express the  $(\partial\phi/\partial t)^2$  term of Eq. (A3) in terms of acoustic pressure. This can readily be done by combining the first-order equation of motion,  $\nabla P = -\rho_0(\partial\mathbf{u}/\partial t)$ , with the definition of the velocity potential to obtain

$$P = \rho_0 \frac{\partial\phi}{\partial t}. \quad (\text{A4})$$

Note that in Eq. (A4) the usual constant of integration has been arbitrarily selected to be equal to the hydrostatic pressure. This is permissible since the definition  $\mathbf{u} = -\nabla\phi$  allows a certain freedom in the choice of the function  $\phi$  (in analogy with the freedom of the choice of "gauge" in electrodynamics). Combining Eqs. (A1)–(A4) produces

$$\square^2 P = -c_0^{-4} \rho_0^{-1} \left[ 1 + \frac{\rho_0}{2} \left( \frac{\partial^2 P}{\partial \rho^2} \right)_{s, \rho = \rho_0} c_0^{-2} \frac{\partial^2 (P)^2}{\partial t^2} \right] + \square^2 \left( \frac{1}{2} \rho_0^{-1} c_0^2 (\Delta \rho)^2 - \frac{1}{2} \rho_0 u^2 - \frac{1}{2} \rho_0 c_0^{-2} \frac{\partial^2}{\partial t^2} (\phi^2) \right). \quad (\text{A5})$$

Since no perturbation expansions have yet been introduced, it is useful to note that Eq. (A5) remains accurate to second order even when first-order terms become small relative to second-order terms. To obtain the simple-source formulation, however, we introduce the perturbation expansion  $P = \epsilon P_1 + \epsilon^2 P_2$  (where  $\epsilon$  is the Mach number and  $\square^2 P_1 = 0$ ).

Equation (A5) may be solved by moving the terms that are under the D'Alembertian operator on the right-hand

side of this equation to the left-hand side. On the left-hand side of this equation we then have  $P_2$  plus additional terms under the D'Alembertian operator. This new equation can now be solved for this new combination, subtracting the additional terms from the solution to obtain  $P_2$ . In practice, the terms under the D'Alembertian operator on the right-hand side of this equation are very small and can usually be neglected. In any case, these terms will clearly be nongrowing contributions to the solution and will quickly be overwhelmed by the growing contributions.

One further remark is worthwhile in discussing the D'Alembertian terms of Eq. (A5). If, in fact, these terms are not negligible in comparison to the predicted value for  $P_2$  obtained in solving this equation, the result thus predicted may very well be in error. This is due to the fact that in such a case it is no longer reasonable to neglect the surface integrals arising from the Green's function solution [as was done in regard to Eq. (5)]. Since accurate boundary values for the second-order pressure are rarely known, it is unlikely that these surface integrals could be properly calculated. Hence, in solving Eq. (A5) via this "lumping" technique, the values given by the D'Alembertian terms on the right-hand sides must always be compared with the predicted value for  $P_2$  in order to insure consistency of the solution. At this point, we assume the D'Alembertian terms on the right-hand side of Eq. (A5) are negligible.

Using the definitions following Eq. (1) we can put Eq. (A5) into the form:

$$\square^2 P_2 = -\rho_0 \left( \frac{\partial q}{\partial t} \right), \quad (\text{A6})$$

which is the simple-source formulation of the nonlinear wave equation.

<sup>1</sup>D. Censor, "Scattering by time-varying obstacles," *J. Sound Vib.* **25**, 101–110 (1972).

<sup>2</sup>P. H. Rogers, "Comments on 'Scattering by time-varying obstacles,'" *J. Sound Vib.* **28**, 764–768 (1973).

<sup>3</sup>J. C. Piquette, "Nonlinear scattering of acoustic waves by vibrating obstacles," Ph.D. thesis, Stevens Institute of Technology (1983). (Also published as NRL Memo. Rep. 5077, issued 1 June 1983.)

<sup>4</sup>P. J. Westervelt, "Parametric acoustic array," *J. Acoust. Soc. Am.* **35**, 535–537 (1963).

<sup>5</sup>J. J. Faran, "Sound scattering by solid cylinders and spheres," *J. Acoust. Soc. Am.* **23**, 405 (1951).

<sup>6</sup>P. M. Morse and K. U. Ingard, *Theoretical Acoustics* (McGraw-Hill, New York, 1968), p. 401.

<sup>7</sup>See Ref. 6, p. 366.

<sup>8</sup>See, for example, D. I. Blokhintsev, *The Acoustics of a Moving Homogeneous Medium*, translated by R. T. Beyer and D. Mintzer (Brown University, Providence, RI, 1952), Sec. 24.

<sup>9</sup>J. C. Piquette and A. L. Van Buren, "Technique for evaluating indefinite integrals involving products of certain special functions," *SIAM J. Math. Anal.* **15**, 845–855 (1984).

<sup>10</sup>L. W. Dean, "Interactions between sound waves," *J. Acoust. Soc. Am.* **34**, 1039 (1962).

<sup>11</sup>M. B. Moffett and J. E. Blue, "Hydrophone nonlinearity measurements," Naval Underwater Systems Center Tech. Memo. No. 801150 (September 1980).

<sup>12</sup>M. B. Moffett and T. A. Henriquez, "Hydrophone nonlinearity measurements," *J. Acoust. Soc. Am.* **72**, 1–6 (1982).

<sup>13</sup>C. Eckart, "Vortices and streams caused by sound waves," *Phys. Rev.* **73**, 68–76 (1948).

<sup>14</sup>P. J. Westervelt, "Scattering of sound by sound," *J. Acoust. Soc. Am.* **24**, 199 (1957).

<sup>15</sup>D. T. Blackstock, "Approximate equations governing finite-amplitude sound in thermoviscous fluids," AFOSR-5223 Suppl. Tech. Rep. (May

1963).

<sup>16</sup>M. J. Lighthill, *Surveys in Mechanics*, edited by G. K. Batchelor and R. M. Davies (Cambridge U. P., Cambridge, UK, 1956), pp. 150–351.